HHS Public Access

Author manuscript

*Kidney Int*. Author manuscript; available in PMC 2014 December 01.

Published in final edited form as:

*Kidney Int*. 2014 June ; 85(6): 1461–1468. doi:10.1038/ki.2013.493.

# A mouse collagen4α4 mutation causing Alport glomerulosclerosis with abnormal collagen α3α4α5(IV) trimers

**Ron Korstanje**[1], **Christina Caputo**[1], **Rosalinda Doty**[1], **Susan Cook**[1], **Roderick Bronson**[1], **Muriel Davisson**[1], and **Jeffrey H. Miner**[2]

[1]The Jackson Laboratory, Bar Harbor, Maine, USA

[2]Renal Division, Washington University School of Medicine, St. Louis, Missouri, USA

## Abstract

A spontaneous mutation termed bilateral wasting kidneys (*bwk*) was identified in a colony of NONcNZO recombinant inbred mice. These mice exhibit a rapid increase of urinary albumin at an early age associated with glomerulosclerosis, interstitial nephritis, and tubular atrophy. The mutation was mapped to a location on Chromosome 1 containing the *Col4a3* and *Col4a4* genes, for which mutations in the human orthologs cause the hereditary nephritis Alport syndrome. DNA sequencing identified a G to A mutation in the conserved GT splice donor of *Col4a4* intron 30, resulting in skipping of exon 30 but maintaining the mRNA reading frame. Protein analyses showed that mutant collagen α3α4α5(IV) trimers were secreted and incorporated into the glomerular basement membrane (GBM), but levels were low, and GBM lesions typical of Alport syndrome were observed. Moving the mutation into the more renal damage-prone DBA/2J and 129S1/SvImJ backgrounds revealed differences in albuminuria and its rate of increase, suggesting an interaction between the *Col4a4* mutation and modifier genes. This novel mouse model of Alport syndrome is the only one shown to accumulate abnormal collagen α3α4α5(IV) in the GBM, as also found in a subset of Alport patients. These mice will be valuable for testing potential therapies, for understanding abnormal collagen IV structure and assembly, for gaining better insights into the mechanisms leading to Alport syndrome and to the variability in the age of onset and associated phenotypes.

## Introduction

Alport syndrome is a human hereditary glomerulonephritis that in most cases results in end-stage renal disease (ESRD).[1] Other clinical symptoms include high-tone sensorineural deafness and ocular defects affecting the lens and the fundus. Alport syndrome is the most common inherited glomerular disease leading to renal failure and is caused by mutations in any one of the genes encoding the α3, α4, or α5 chains of type IV collagen (*COL4A3*,



Correspondence: Ron Korstanje, The Jackson Laboratory, 600 Main Street, Bar Harbor, Maine 04609, USA. ron.korstanje@jax.org; or Jeffrey H. Miner, Renal Division 8126, Washington University School of Medicine, 660 S. Euclid Ave., St. Louis, Missouri 63110, USA. minerj@wustl.edu.

Disclosure

All the authors declared no competing interests.

*COL4A4*, and *COL4A5*, respectively).[2] α3α4α5(IV) heterotrimers are secreted by podocytes[3,4] and polymerize to form the major collagen IV network of the GBM.[5]*COL4A5* is located on the X Chromosome (Chr) and is mutated in X-linked Alport syndrome, whereas mutations in *COL4A3* and *COL4A4*, which are located on human Chr 2, lead to autosomal recessive Alport syndrome and, in rare cases, to autosomal dominant Alport syndrome.[6]

All collagen IV α chains have a large central triple helical collagenous domain with multiple interruptions, an NH2-terminal noncollagenous domain termed 7S, and a COOH-terminal noncollagenous domain termed NC1. The NC1 domain promotes both heterotrimerization of α chains to form a protomer and association of two protomers to form a macromolecule containing six NC1 domains. These six NC1 domains constitute a collagenase-resistant structure called a hexamer. Hexamer formation, together with interactions among 7S domains from four different protomers, contribute to collagen IV network polymerization.[5]

Because the GBM functions normally in Alport patients for several to many years, it is possible that blocking the events that trigger initiation of overt disease might arrest Alport syndrome in its pre-pathogenic state. Therefore, understanding disease initiation and progression and the factors that are involved in these processes could lead to therapeutic interventions.[7] Animal models can play a critical role in achieving this understanding.[8]

In the past two decades, knockout (KO) mice for *Col4a3*[9,10], *Col4a4*[11], *Col4a5*[12] and both *Col4a3* and *Col4a4* together[13] have been generated and characterized. Studying these mice has led to an understanding of several important aspects of the disease and its progression, such as the α5/α6 switch, in which the disease in *Col4a3* KO mice can be partially delayed by ectopic deposition of collagen α5α5α6(IV) protomers in the GBM; this feature is highly dependent on genetic background.[8] Another important finding is the presence of modifier genes that influence the GBM ultrastructure and mean age at renal failure in *Col4a3* KO mice.[14]

In 2002 a spontaneous mutant was identified in a colony of severely obese NONcNZO4/Lt (RCS-4) recombinant congenic mice.[15] The mutant was identified because of its leanness. Subsequent phenotyping showed chronic nephritis, and the mutation was named bilateral wasting kidneys (*bwk*). We now report mapping the *bwk* mutation to Chr 1 and identify *Col4a4* as the mutated gene. Immunohistochemical analyses revealed this mutant to be the first mouse model of Alport syndrome with detectable collagen α3α4α5(IV) in the GBM. However, because the collagen IV is abnormal, the typical GBM lesions observed in Alport syndrome are present, consistent with the observed progression to ESRD.

## Results

### Origin of the *bwk* mutation

The bilateral wasting kidneys (*bwk*) mutant phenotype, determined by breeding to be autosomal recessive, was observed in the NONcNZO4/Lt (RCS-4) recombinant congenic strain at generation N2F10. Mutants on this inbred genetic background began to appear leaner than RCS-4 mice one to two weeks after weaning and died between 8 and 10 weeks

of age. At autopsy, the kidneys of affected mice appeared pale and pitted. Due to inbreeding depression, mice of this mutant subline were crossed one generation to NON/ShiLtJ (NON) mice; offspring of this cross were then crossed with N2F12 *bwk/bwk* cousins. Since then, the *bwk* mutation has been maintained homozygous on this inbred genetic background by sibling or cousin matings.

### Characterization of *bwk* mutant mice

The *bwk* mutation causes ESRD associated with glomerulosclerosis, synechiae (adhesions of the glomerular tuft to Bowman's capsule), glomerular crescents, tubular protein casts, tubular atrophy, and tubulointerstitial nephritis as major histopathologic components (Figure 1 and data not shown). The expanded interstitium, which appears to include inflammatory cells, eventually replaces or impinges on many of the tubules (Figure 1). To determine whether the inflammatory phenotype might be caused by T or B cells, we crossed *bwk* mice to B6.129S7-*Rag1*$^{tm1Mom}$/J (*Rag1* KO) mice. The presence of a similar kidney phenotype in *bwk/bwk; Rag1*$^{tm1Mom}$*/Rag1*$^{tm1Mom}$ mice (data not shown) showed that the inflammation was not due to exclusively T or B cells, which are absent in *Rag1* KO mice.[16] *Rag1* KO mice still have functional cells of the innate immune system, so the inflammatory cells in the double knockout kidneys must be of "innate immunity" type, as opposed to "adaptive (T and B cells) immunity" type.

Consistent with the observed histopathology (Figure 1), *bwk/bwk* mice rapidly developed high albuminuria. A time course of albumin-to-creatinine ratios (ACR) showed an already slightly elevated ACR at 4 weeks compared to controls, which increased in the course of only six weeks to 3400 mg/g in both males and females (Figure 2, top panels).

### Mapping of *bwk* to a region on Chr 1

An initial genome-wide scan of DNA markers in progeny of a backcross between CAST and *bwk* allowed us to map the mutation to a 16 Mb region on Chr 1 between *D1Mit46* and *D1Mit488*. Subsequent fine mapping in an intercross with CAST narrowed the region to a 4.2 Mb interval (Figure 3A) containing 29 genes, including *Col4a3* and *Col4a4*. Because of their known roles in kidney disease in both mice and humans (Alport syndrome), these genes were deemed to be excellent candidates for harboring the *bwk* mutation.

### A complementation test excludes *Col4a3* as a candidate gene

To directly test whether *bwk* is a mutation in *Col4a3*, we performed a complementation test in which *Col4a3*+/− females were mated to *bwk/bwk* males. This cross produced two distinct groups of mice: those with a *Col4a3* KO allele and a *bwk* allele (n=15), and those with one obligate *Col4a3* wild-type allele and a *bwk* allele (n=5). As *bwk* is recessive, mice in the first group were expected to develop albuminuria only if *bwk* resides in the *Col4a3* gene, while those in the second group were expected not to show any albuminuria. Neither group showed either elevated albuminuria or renal damage at any time point (data not shown), indicating that *bwk* could not be a mutation in *Col4a3*. This left *Col4a4* as the prime candidate gene.

### Identification of a mutation in *Col4a4* and its effects on *Col4a4* mRNA and protein

Sequencing of *Col4a4* exons, intron splice sites, and the 3′ UTR revealed a G to A point mutation in the first base following the 3′ end of exon 30 (i.e., the first base of intron 30; Figure 3B). This mutation, which was not detected in any other strains, affects the GT consensus splice donor of intron 30 and should therefore prevent proper splicing of the mRNA.

To investigate the effect of the mutation on *Col4a4* mRNA, we performed RT-PCR using primers from exons 28 and 32 on whole kidney RNA. The primers (Figure 3C) generated the expected product from WT RNA but only a shorter product from *bwk* mutant RNA (Figure 3D). Sequencing of the short PCR product showed a direct splice from exon 29 to exon 31, indicating a clean skip of exon 30 (Figure 3C, E). Quantitative real-time RT-PCR using primers from *Col4a4* exons 3' of exon 30 showed an average 55% reduction ($P<0.0006$ by Student's two-tailed $t$ test) in the level of transcript in mutant vs. WT whole kidney RNA samples. We therefore suggest that the alternative splicing was not 100% efficient and that a large subset of mutant transcripts retained intron 30 and were degraded due to nonsense-mediated mRNA decay.[17]

Because the skipped exon 30 is 171 bp and encodes 57 amino acids of the collagenous domain (amino acids 841-897), the reading frame of the mutant mRNA should be maintained and should produce a 1625 amino acid protein rather than the full length 1682 amino acid protein. Such a protein may or may not be capable of assembling with the α3 and α5 chains to form a protomer. Immunohistochemistry on WT and *bwk/bwk* kidneys using an antibody to the NC1 domain of α4 showed a reduction in the mutant GBM, but α4 was present (Figure 4a-c, red). Double staining with an antibody to α2, which normally labels primarily the mesangial matrix, also labeled the GBM (Figure 4a-f, green), a typical finding in Alport syndrome.[18] Staining with a monoclonal antibody[19] whose epitope requires proper assembly of α3α4α5(IV) NC1 domains into hexamers was weaker vs. WT, but clearly positive in the mutant (Figure 4g-i). This confirmed that some mutant α4 was synthesized and capable of at least partial assembly with α3 and α5 into protomers that could interact with each other via their NC1 domains to form hexamers. However, the low levels suggest a significant amount of posttranslational degradation. Electron microscopy showed the characteristic GBM splitting, thickening, and basket-weave pattern found in Alport syndrome (Figure 5E-H).

Since patients with Alport syndrome are often diagnosed with ear and eye problems, we tested the *bwk* mice for these characteristics. No histological differences were observed for the eyes, and a hearing evaluation (by measuring Auditory Brainstem Response) did not show any deviations from WT animals (data not shown).

### Introduction of *bwk* into different genetic backgrounds leads to phenotypic differences

Studies using the *Col4a3* KO have demonstrated how the genetic background can impact kidney disease severity and its rate of progression to ESRD.[14] We therefore introduced the *bwk* mutation into the 129S1/SvImJ (129S1) and into the more renal damage prone DBA/2J

(D2) genetic backgrounds by backcrossing. D2 mice are relatively susceptible to increased ACR[20] and at 12 weeks of age have a higher ACR compared to NONcNZO or 129S1 mice.

Animals homozygous for *bwk* in the D2 genetic background showed a dramatic increase in ACR, with levels around 7300 mg/g in females and 8700 mg/g in males at 12 weeks of age (Figure 2, bottom panels). In the 129S1 background, the mutants exhibited lower ACR levels in the 12-week timeframe compared to the D2 background, but levels were higher than those observed in the NONcNZO background (3000 mg/g in females and 5000 mg/g in males) (Figure 2, middle panels). Histological differences in the two genetic backgrounds were found at 6 and 9 weeks of age (Figure 5A-D); most notable was that tubular protein casts were more readily detected at 6 weeks of age on the D2 background, consistent with the higher ACRs vs. 129S1 (Figure 2). Quantitation of GBM lesions by ultrastructural analyses (Figure 5E-H) revealed reductions in the percentage of normal GBM stretches by 6 weeks of age on both genetic backgrounds (Table 1); but this analysis, albeit limited, did suggest that there are more extensive lesions on the D2 vs. 129S1 background at 6 weeks of age, though not at 9 weeks of age. As these differences in both ACR and histopathology correlated with the genetic background, there are likely to be interactions between *bwk* and modifier genes, especially at early stages. At 12 weeks of age, mutant kidneys of both backgrounds showed signs of severe ESRD and were indistinguishable (data not shown).

## Discussion

Alport syndrome is caused by mutations in *COL4A3*, *COL4A4*, or *COL4A5*. Although the observed phenotypes fall within a relatively well-defined disease spectrum, they can be rather complicated. Importantly, there can be substantial variability in phenotype among patients—even those carrying the identical collagen IV mutation.[21,22] In addition, many patients seem to have normal kidney function for a long time, with significant differences in disease onset.[1] A better understanding of the basis for this variability and the process of disease initiation is necessary to develop methods to block disease onset and to identify therapies to ameliorate or even reverse the disease phenotype. Animal models are crucial for this process, and mice with various *Col4a3/a4/a5* mutations have already shown their value by leading to important discoveries about Alport syndrome, though some have been controversial.[23]

In this report we describe a novel mutant allele of the mouse *Col4a4* gene, *Col4a4*$^{bwk}$. This spontaneous mutation causes a rapid increase of urinary albumin at an early age that is associated with GBM thickening and splitting, glomerulosclerosis with synechiae, tubulointerstitial nephritis, and progression to ESRD. The mutation changes the first base of intron 30 from G to A and therefore affects the consensus splice donor site. This results in skipping of exon 30 and absence of 57 amino acids from the collagenous domain of α4. However, immunohistochemical results suggested that this abnormal protein was able to assemble with α3 and α5 to form protomers that were secreted into the GBM and capable of protomer-protomer interactions to form typical NC1 hexamers, though levels were lower than normal. To our knowledge, this is the first animal model of Alport syndrome with detectable α3, α4, and α5(IV) chains in the GBM, a situation also observed in a subset of patients.[24,25] These mice will therefore be useful for better understanding why the collagens

are nonfunctional and whether development of specific therapies might be feasible for this class of patients. It is worth noting here that 17% of entries in the Alport Syndrome *COL4A5* Variant Database[26] (http://www.arup.utah.edu/database/ALPORT/ALPORT_welcome.php) are splice site mutations, and there is a recent report of two pathogenic splice site mutations in human *COL4A4* that affect the first base (G) of introns 22 and 28, respectively.[27]

The mean age of death of the *bwk/bwk* mice was ~124 days on the NONcNZO background and ~84 days on the DBA/2J background. It is not possible at this point to determine whether there is a difference in survival in *Col4a3* KO vs. *Col4a4*$^{bwk/bwk}$ mice, as different genetic backgrounds were used in the studies, but it is clear that there is a strong genetic background effect influencing both ACRs and longevity. Now that mutants for both genes are available on multiple genetic backgrounds, it may be possible to localize modifier loci through linkage analysis by crossing the different strains.

The discovery of the *Col4a4*$^{bwk}$ mutation and our studies using different genetic backgrounds provide a critical step towards fully understanding the mechanisms in Alport syndrome and development of treatments to extend normal GBM function and delay or prevent the trigger that sets off the initiation of renal damage and end-state renal disease. In addition, the availability of mice that secrete abnormal α3α4α5(IV) trimers will provide a new tool for investigating the biochemistry of abnormal GBM collagen IV assembly and function.

## Materials and methods

### Mice, breeding, and urinalysis

NON/ShiLtJ, DBA/2J (D2), CAST/EiJ (CAST), 129S1/SvImJ (129S1), 129-*Col4a3*$^{tm1Dec}$/J, and B6.129S7-*Rag1*$^{tm1Mom}$/J mice were obtained from The Jackson Laboratory (Bar Harbor, ME). NON;NZO-*bwk*/J were kindly provided by Dr. Edward Leiter (The Jackson Laboratory). NON/ShiLtJ (NON) mice were used as controls; littermate controls were not available because the *bwk* mutation was maintained in a homozygous state. All mice were housed in a climate-controlled facility with a 14-hour:10-hour light-dark cycle and provided free access to a standard rodent chow diet containing 6% fat by weight (5k52 LabDiet, Brentwood, MO) and acidified water.

In an initial genetic mapping cross, CAST/EiJ (CAST) females were crossed with homozygous NON;NZO-*bwk*/J males, and F1 female offspring were subsequently backcrossed to homozygous NON;NZO-*bwk*/J males. To fine map the mutation, CAST females were mated to *bwk/bwk* males, and the F1 offspring were intercrossed to produce the F2 generation. 378 F2 mice were tested for albuminuria at 6, 8, 10, and 12 weeks, and kidneys were collected for histology at 14 weeks of age. Initially we used simple sequence length polymorphic (SSLP) markers that were polymorphic between CAST and NONcNZO4/Lt. Once the region was narrowed to a 16 Mb locus on Chr 1 that was homozygous NON in affected backcross mice, the region was fine-mapped in the F2 mice using SSLP and SNP markers polymorphic between CAST and NON according to the Mouse Phenome Database (phenome.jax.org).

The *bwk* mutation was introduced into the 129S1 and D2 strain backgrounds by backcrossing heterozygous *bwk* males to 129S1 and D2 females, respectively, for 8 generations, and by then backcrossing heterozygous *bwk* females to male 129S1 and D2 animals to move the 129S1 and D2 Y chromosomes into the respective congenic lines. This was followed by intercrossing a heterozygous male and female and selecting *bwk/bwk* animals to start the congenic colonies.

Urinary albumin and creatinine concentrations in spot urine samples were determined with a Beckman Synchron CX5 Chemistry Analyzer. All animal experiments were performed in accordance with the National Institutes of Health Guide for the Care and Use of Laboratory Animals (National Research Council) and were approved by The Jackson Laboratory's Animal Care and Use Committee.

### Sequencing

Genomic DNA from NON and *bwk* mice was isolated from tail clips. *Col4a4* primers were designed to cover the promoter, exons with flanking intronic segments, and 3′UTR using the C57BL/6J sequence obtained from Ensembl (NCBI Build 37). PCR products were sequenced in both directions on an Applied Biosystems 3730. Sequences were aligned using the sequence analysis program Sequencher 4.8 and analyzed for differences.

### Analysis of *Col4a4* mRNA

RNA was isolated from *bwk/bwk* and control kidneys using the Trizol Plus method. Total RNA was reverse transcribed and subjected to PCR using a forward primer in exon 28 (5'-TTCCAGGAGCACCAGGCATG-3') and a reverse primer in exon 32 (5'-CCTGAGAACCCACCATCTCCTG-3'). The amplicon derived from the mutant allele was purified and sequenced with the forward primer. For quantitative real-time RT-PCR, a mouse Col4a4 QuantiTect Primer Assay was purchased from Qiagen (QT00287392) and used with Applied Biosystems Fast SYBR Green Master Mix on an Applied Biosystems 7900HT Fast Real-Time PCR System. The primers amplify a 118 bp amplicon approximately 1000 bp 3' of exon 30. Hprt primers were used for normalization.

### Light and electron microscopy and quantitation of GBM ultrastructure

Kidneys from *bwk/bwk* and NON mice were collected for histological analysis. Bouin's-fixed tissues were paraffin embedded, sectioned at 3 μm, and stained with periodic acid Schiff or hematoxylin & eosin (H&E). For transmission electron microscopy (TEM), tissues were fixed, embedded in plastic, sectioned, and stained as previously described.[28] To quantitate the extent of GBM lesions, stretches of total and normal GBM lengths were measured, and the percent normal was calculated. At least 24 capillary loops from 2 different glomeruli were analyzed for each mouse.

### Immunohistochemistry

Ten μm sections of kidneys frozen in OCT were cut on a cryostat and fixed and denatured with urea-glycine as described.[29] Primary antibodies have been described: rabbit anti-COL4A4 NC1 domain;[29] mouse anti-collagen α3α4α5(IV) NC1 hexamer[19] (clone 26-20, a

gift from Dr. Bogdan Borza, Vanderbilt University); and rat anti-COL4A2 NC1[30] (clone H22, a gift from Yoshikazu Sado, Shigei Medical Research Institute, Okayama, Japan).

## Acknowledgements

We thank Edward H. Leiter and Peter Reifsnyder for providing the original *bwk* mutant strain, Coleen Kane, Gloriosa Go, Jennifer Richardson, Mohammad Hashim, and Jeanette Cunningham for technical assistance, Louise Dionne for breeding the mice, Joanne Currer for writing assistance, the Washington University O'Brien Center for Kidney Disease Research (supported by P30DK079333) for electron microscopy, and The Jackson Laboratory Cancer Center Core Grant (P30CA034196). This work was supported by grants from the NIH (R01DK069381 to RK; R01DK064674 and P40RR001183 to MTD; R01DK078314 and R21DK095419 to JHM), and in part by a grant from the Alport Syndrome Foundation (to JHM).

## References

1. Savige J, Gregory M, Gross O, et al. Expert guidelines for the management of Alport syndrome and thin basement membrane nephropathy. J Amer Soc Nephrol. 2013; 24:364–375. [PubMed: 23349312]
2. Hudson BG, Tryggvason K, Sundaramoorthy M, et al. Alport's syndrome, Goodpasture's syndrome, and type IV collagen. N Engl J Med. 2003; 348:2543–2556. [PubMed: 12815141]
3. Abrahamson DR, Hudson BG, Stroganova L, et al. Cellular origins of type IV collagen networks in developing glomeruli. J Am Soc Nephrol. 2009; 20:1471–1479. [PubMed: 19423686]
4. Heidet L, Cai Y, Guicharnaud L, et al. Glomerular expression of type IV collagen chains in normal and X-linked Alport syndrome kidneys. Am J Pathol. 2000; 156:1901–1910. [PubMed: 10854213]
5. Hudson BG. The molecular basis of Goodpasture and Alport syndromes: beacons for the discovery of the collagen IV family. J Am Soc Nephrol. 2004; 15:2514–2527. [PubMed: 15466256]
6. van der Loop FT, Heidet L, Timmer ED, et al. Autosomal dominant Alport syndrome caused by a COL4A3 splice site mutation. Kidney Int. 2000; 58:1870–1875. [PubMed: 11044206]
7. Cosgrove D. Glomerular pathology in Alport syndrome: a molecular perspective. Pediatr Nephrol. 2012; 27:885–890. [PubMed: 21455721]
8. Cosgrove D, Kalluri R, Miner JH, et al. Choosing a mouse model to study the molecular pathobiology of Alport glomerulonephritis. Kidney Int. 2007; 71:615–618. [PubMed: 17290292]
9. Miner JH, Sanes JR. Molecular and functional defects in kidneys of mice lacking collagen alpha 3(IV): implications for Alport syndrome. J Cell Biol. 1996; 135:1403–1413. [PubMed: 8947561]
10. Cosgrove D, Meehan DT, Grunkemeyer JA, et al. Collagen COL4A3 knockout: a mouse model for autosomal Alport syndrome. Genes Dev. 1996; 10:2981–2992. [PubMed: 8956999]
11. Arnold CN, Xia Y, Lin P, et al. Rapid identification of a disease allele in mouse through whole genome sequencing and bulk segregation analysis. Genetics. 2011; 187:633–641. [PubMed: 21196518]
12. Rheault MN, Kren SM, Thielen BK, et al. Mouse model of X-linked Alport syndrome. J Am Soc Nephrol. 2004; 15:1466–1474. [PubMed: 15153557]
13. Lu W, Phillips CL, Killen PD, et al. Insertional mutation of the collagen genes Col4a3 and Col4a4 in a mouse model of Alport syndrome. Genomics. 1999; 61:113–124. [PubMed: 10534397]
14. Andrews KL, Mudd JL, Li C, et al. Quantitative trait loci influence renal disease progression in a mouse model of Alport syndrome. Am J Pathol. 2002; 160:721–730. [PubMed: 11839593]
15. Reifsnyder PC, Leiter EH. Deconstructing and reconstructing obesity-induced diabetes (diabesity) in mice. Diabetes. 2002; 51:825–832. [PubMed: 11872687]
16. Mombaerts P, Iacomini J, Johnson RS, et al. RAG-1-deficient mice have no mature B and T lymphocytes. Cell. 1992; 68:869–877. [PubMed: 1547488]
17. Hentze MW, Kulozik AE. A perfect message: RNA surveillance and nonsense-mediated decay. Cell. 1999; 96:307–310. [PubMed: 10025395]
18. Kashtan CE, Kim Y. Distribution of the α1 and α2 chains of collagen IV and of collagens V and VI in Alport syndrome. Kidney Int. 1992; 42:115–126. [PubMed: 1635341]

19. Heidet L, Borza DB, Jouin M, et al. A human-mouse chimera of the alpha3alpha4alpha5(IV) collagen protomer rescues the renal phenotype in Col4a3-/-Alport mice. Am J Pathol. 2003; 163:1633–1644. [PubMed: 14507670]
20. Sheehan S, Tsaih SW, King BL, et al. Genetic analysis of albuminuria in a cross between C57BL/6J and DBA/2J mice. Am J Physiol Renal Physiol. 2007; 293:F1649–1656. [PubMed: 17804484]
21. Barker DF, Denison JC, Atkin CL, et al. Common ancestry of three Ashkenazi-American families with Alport syndrome and COL4A5 R1677Q. Hum Genet. 1997; 99:681–684. [PubMed: 9150741]
22. Barker DF, Pruchno CJ, Jiang X, et al. A mutation causing Alport syndrome with tardive hearing loss is common in the western United States. Am J Hum Genet. 1996; 58:1157–1165. [PubMed: 8651292]
23. Gross O, Borza DB, Anders HJ, et al. Stem cell therapy for Alport syndrome: the hope beyond the hype. Nephrol Dial Transplant. 2009; 24:731–734. [PubMed: 19110486]
24. Gubler MC. Inherited diseases of the glomerular basement membrane. Nat Clin Pract Nephrol. 2008; 4:24–37. [PubMed: 18094725]
25. Gubler M-C, Knebelmann B, Beziau A, et al. Autosomal recessive Alport syndrome: Immunohistochemical study of type IV collagen chain distribution. Kidney Int. 1995; 47:1142–1147. [PubMed: 7783412]
26. Crockett DK, Pont-Kingdon G, Gedge F, et al. The Alport syndrome COL4A5 variant database. Hum Mutat. 2010; 31:E1652–1657. [PubMed: 20574986]
27. Zhang Y, Wang F, Ding J, et al. Genotype-phenotype correlations in 17 Chinese patients with autosomal recessive Alport syndrome. Am J Med Genet A. 2012; 158A:2188–2193. [PubMed: 22887978]
28. Noakes PG, Miner JH, Gautam M, et al. The renal glomerulus of mice lacking slaminin/laminin beta 2: nephrosis despite molecular compensation by laminin beta 1. Nat Genet. 1995; 10:400–406. [PubMed: 7670489]
29. Miner JH, Sanes JR. Collagen IV α3, α4, and α5 chains in rodent basal laminae: Sequence, distribution, association with laminins, and developmental switches. J Cell Biol. 1994; 127:879–891. [PubMed: 7962065]
30. Sado Y, Kagawa M, Kishiro Y, et al. Purification and characterization of human nephritogenic antigen that induces anti-GBM nephritis in rats. J Pathol. 1997; 182:225–232. [PubMed: 9274535]

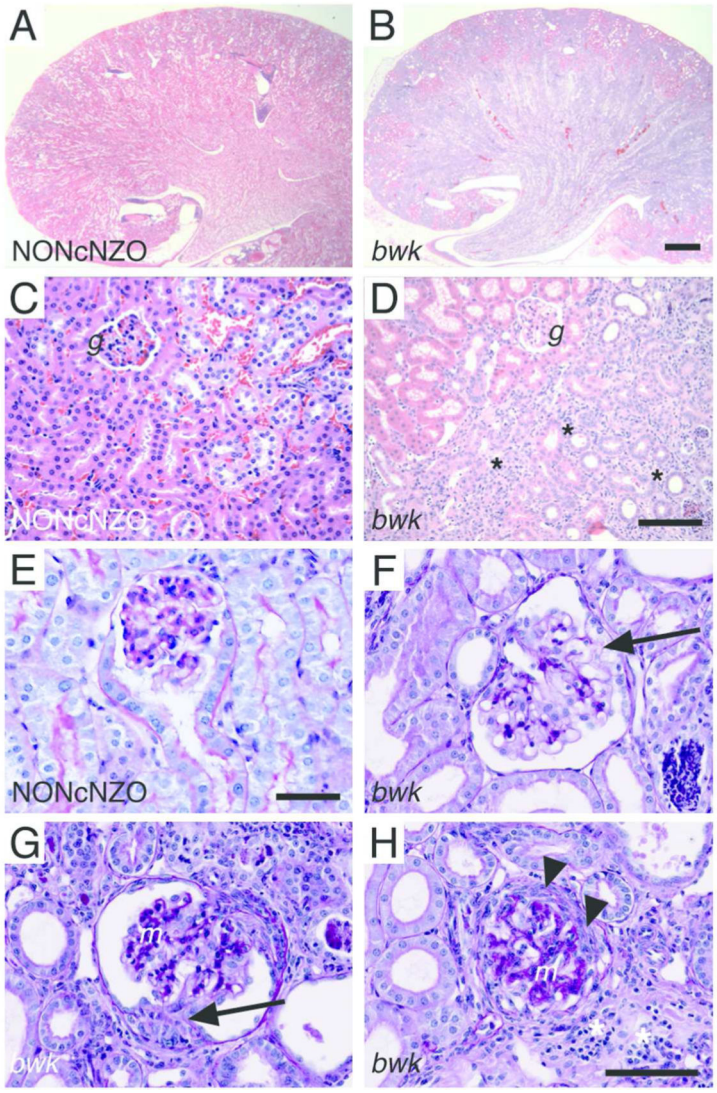


**Figure 1. Renal pathology of NON;NZO-*bwk*/J mice at 3 months of age**

(A, C, E) Images of control kidney sections stained with H&E (A, C) or PAS (E). (B, D, F-H) Images of *bwk* mutant kidney stained with H&E (B, D) or PAS (F-H). The mutant kidneys were much more cellular than the controls due to diffuse infiltrates of inflammatory cells (asterisks). Many mutant tubules were either dilated or atrophic as compared with control tubules. Although some glomeruli were well preserved (F), synechiae (arrows in F and G) and fibrocellular crescents (arrowheads in H) were evident in some mutant glomeruli. Expansion of the mesangial matrix (m in G and H) was also observed. g, glomerulus. Bar in B, 1 mm for A and B; in D, 75 μm for C and D; in E, 50 μm for E; in H, 75 μm for F-H.

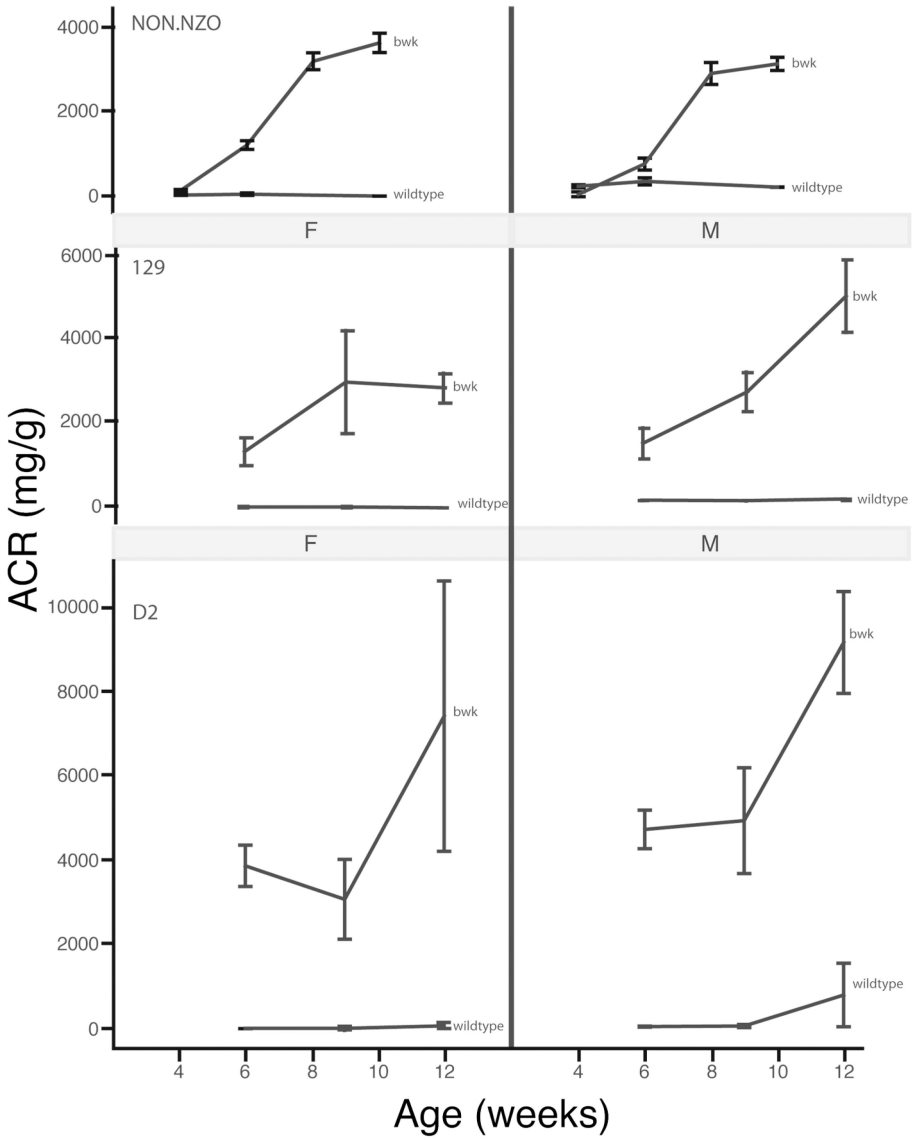


**Figure 2. Progression of increased albumin-to-creatinine ratios in *bwk* mice on three genetic backgrounds**

Alubmin-to-creatinine ratios were determined at various time points in homozygous NON;NZO-*bwk*/J, D2-*bwk*/J, and 129S1-*bwk*/J mice vs. wild-type in both males and females, as indicated. Each group contained 5 animals. A *t*-test was used to determine significant differences between mutant and WT mice for each time point. A * indicates a significant difference of $P<0.01$. Ratios in D2 males were found to be the highest.

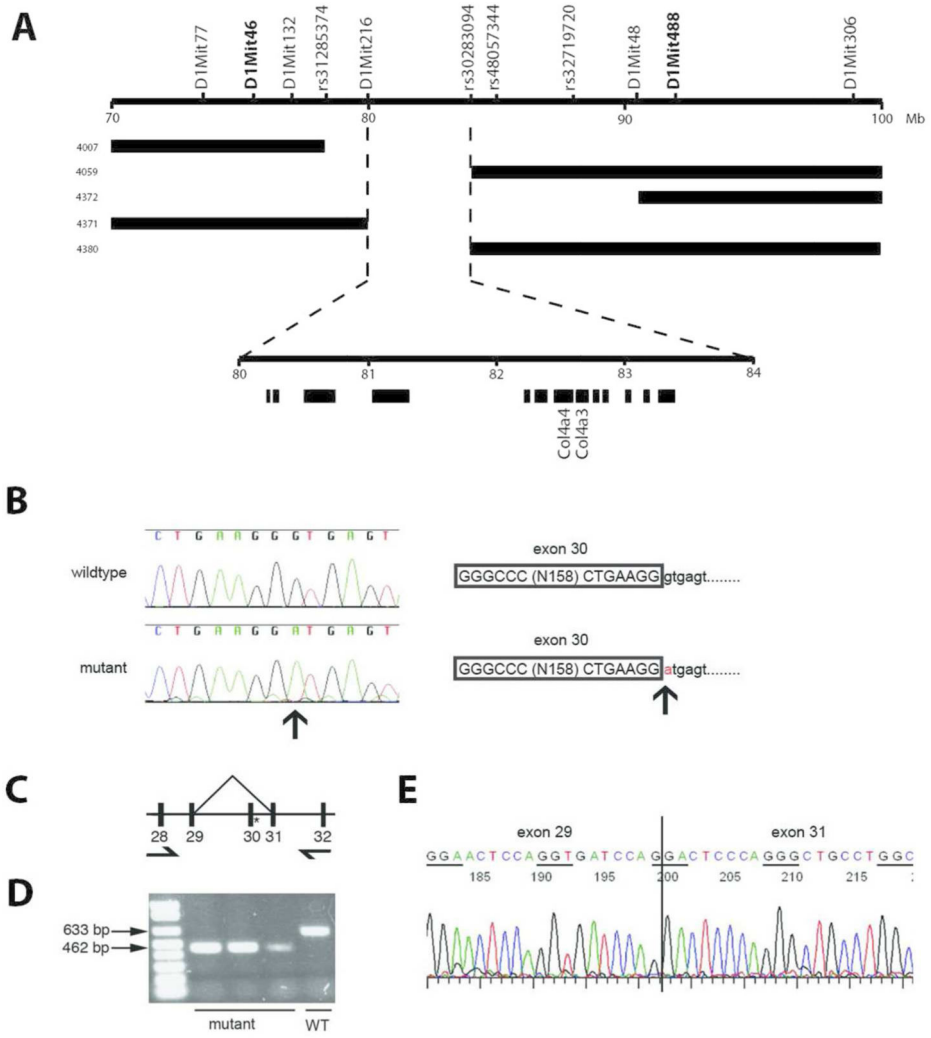


**Figure 3. Mapping of *bwk* and molecular analyses of the *Col4a4*$^{bwk}$ gene and mRNA**

(A) The initial genome-wide scan using SSLP markers mapped the mutation to a region between *D1Mit46* and *D1Mit488* on Chr 1. Additional genotyping using SNP markers narrowed the critical region to 4.2 Mb. Numbers on the left represent the IDs of the mice in the cross that had a crossover event in the region. Black bars indicate the region that is excluded because affected mice were homozygous CAST or heterozygous in this region. (B) Sequencing revealed a mutation (arrows) in the 5' splice site of *Col4a4* intron 30. (C) Primers from *Col4a4* exons 28 and 32 were used for RT-PCR. (D) Agarose gel electrophoretic analysis of RT-PCR products obtained from *bwk/bwk* mutant and WT whole kidney RNA, as indicated. The mutant products were shorter than WT. (E) Sanger sequencing analysis of the mutant RT-PCR product revealed a direct splice from exon 29 to exon 31, as indicated in (C); glycine codons are underlined to show maintenance of the reading frame.

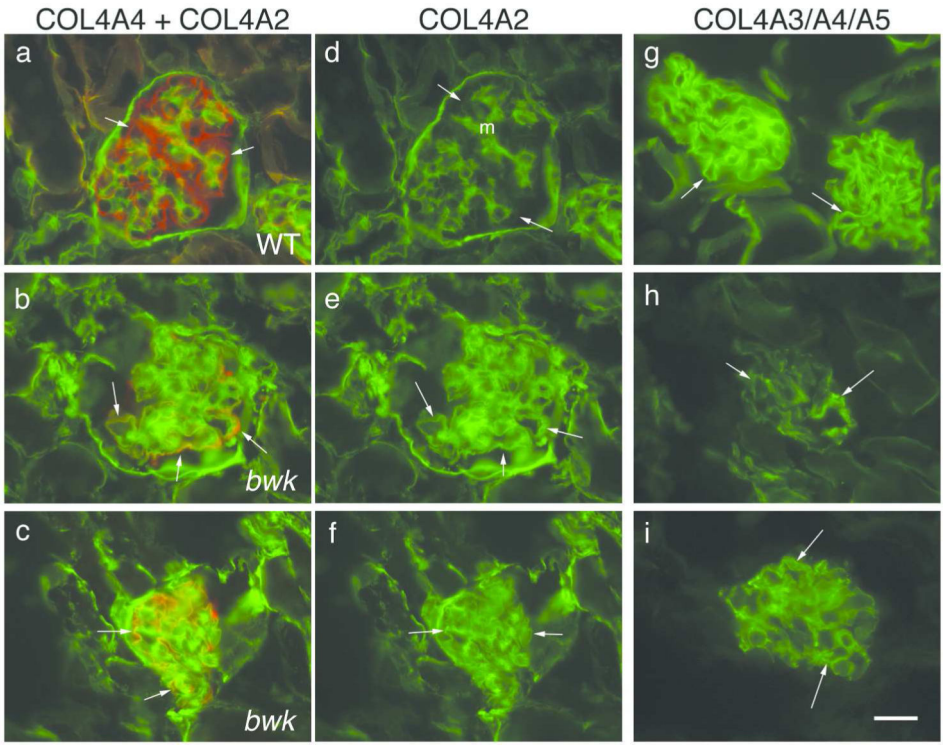


**Figure 4. Immunohistochemical analysis of collagen IV chains in the GBM using epitope-specific antibodies**

(a-c) Collagen α4(IV) (red) was easily detected in the WT control GBM (arrows in a), but levels were reduced in the *bwk* mutants at ten (b) and five (c) weeks of age. Sections were double stained for collagen α2(IV) in green; green channel images are shown separately in d-f. COL4A2 is normally concentrated in the mesangial matrix (m) and weak in GBM (arrows in d), but it was increased in *bwk* GBM (arrows in e and f). (g-i) An antibody specific for assembled collagen α3α4α5(IV) hexamers stained GBM brightly in the WT (arrows in g) but more weakly in *bwk* (arrows in h and i). Bar in i, 20 μm for a-i.

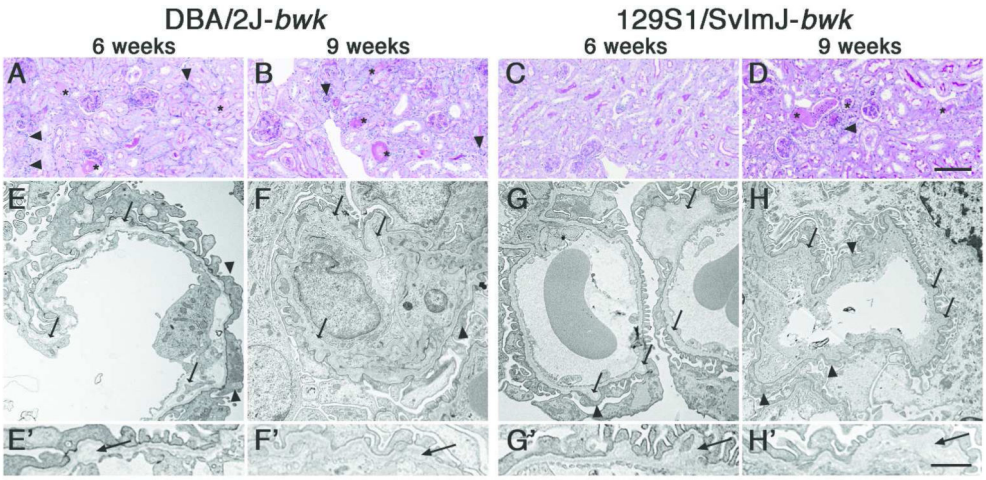


**Figure 5. Alport syndrome-like pathologies in D2- and 129S1-*bwk* kidneys at 6 and 9 weeks of age**

(A-D) PAS staining of homozygous DBA/2J-*bwk* and 129S1/SvImJ-*bwk* kidneys showed early onset protein casts (asterisks) and mild inflammatory cell infiltration (arrowheads) at 6 weeks of age in D2 but not in 129S1 (A and C). By 9 weeks, protein casts, inflammatory cells, tubular atrophy, and glomerular lesions were apparent on both strain backgrounds (B and D). Bar in D, 100 μm for A-D. (E-H) Electron micrographs of *bwk* mutant GBM at 6 and 9 weeks revealed human Alport syndrome-like lesions, including GBM thickening (arrows) and podocyte foot process effacement. Bar in H', 2 μm for E-H; 1 μm for E'-H'.

## Table 1

Quantitation of the percentage of normal GBM in WT and *bwk* mutant mice

| Strain | Age (weeks) | Genotype | % Normal GBM |
|---|---|---|---|
| DBA/2J | 6 | WT | 99.7 |
| | 6 | *bwk* | 70.4 |
| | 9 | WT | 99.8 |
| | 9 | *bwk* | 71.4 |
| 129S1/SvImJ | 6 | WT | 100 |
| | 6 | *bwk* | 85.7 |
| | 6 | *bwk* | 89.5 |
| | 9 | WT | 99.6 |
| | 9 | *bwk* | 72.4 |

Each entry represents an individual mouse